Optical subpicosecond nonvolatile switching and electron-phonon coupling in ferroelectric materials

Nian-Ke Chen,[1,*] Junhyeok Bang,[2,*] Xian-Bin Li [1,†] Xue-Peng Wang,[1] Dan Wang,[3] Qi-Dai Chen,[1]
Hong-Bo Sun,[1,4,‡] and Shengbai Zhang [5,§]

[1]*State Key Laboratory of Integrated Optoelectronics, College of Electronic Science and Engineering, Jilin University,
Changchun 130012, China*
[2]*Department of Physics, Chungbuk National University, Chungbuk 28644, Republic of Korea*
[3]*Department of Materials Science and Engineering, Rensselaer Polytechnic Institute, Troy, New York 12180, USA*
[4]*State Key Lab of Precision Measurement Technology and Instruments, Department of Precision Instrument,
Tsinghua University, Beijing 100084, China*
[5]*Department of Physics, Applied Physics, and Astronomy, Rensselaer Polytechnic Institute, Troy, New York 12180, USA*

Direct optical ferroelectric switching (FE switch) has the advantage of being ultrafast over the traditional FE switch, which relies on domain nucleation and growth. However, how to realize nonvolatility in such an optical FE switch poses a serious challenge. Time-dependent density-functional theory molecular dynamics study reveals that subpicosecond nonvolatile FE switches can be realized in GeTe and PbTiO₃. While optical tuning of the transition barrier and initiation of a directional atomic motion are crucial, the dephasing of the excited state holds the key for the realization of nonvolatility.

I. INTRODUCTION

Nonvolatile memory is at the heart of modern electronics. Various fundamental physical properties have been deployed to realize such a functionality, as in ferroelectric random access memory (FeRAM), phase-change random access memory (PCRAM), resistive random access memory (RRAM), spin-transfer torque magnetic random access memory (STT MRAM), and digital video disk random access memory (DVD RAM) [1–5]. Moreover, nonvolatile memory with ultrafast speed and low power consumption is urgently required nowadays for big data and artificial intelligence applications. One drawback in these technologies lies, however, in the relatively long time required for data writing, i.e., hundreds of picoseconds or tens of nanoseconds. It happens because phase change or ferroelectric switching often takes place via a random nucleation and growth mechanism, or via a domain-wall migration.

In particular, FeRAM relies on ferroelectric switching (FE switch), which is an inversion in the direction of spontaneous polarization of a ferroelectric [6]. The control of the FE switch by an external field has been an enduring subject for more than 70 years [6–8]. Recently, optical control of the FE switch also attracted considerable attention for its significance in light-matter interactions such as in the photovoltaic effect [9–11], photostriction effect [12,13], and domain pinning and domain-wall movement effect [14,15], and for its potentials in optical memory, remote control, and light-induced domain engineering [16,17].

Regarding the optical control, it has been suggested that the electric field associated with the light plays a key role. For example, a continuous-wave (cw) ultraviolent (UV) laser can induce a temperature gradient in LiNbO₃ and a subsequent field to drive the FE switch [18]. For BaTiO₃, a cw UV light can produce charge separation at the MoS₂/BaTiO₃ interface and a subsequent electric field to drive a FEswitch [19]; a cw laser can also trigger the motion of domain walls by acting on their charges and subsequently a FE switch [20]. For BiFeO₃, on the other hand, a laser pulse can lead to a local electric field due to the photovoltaic effect, which is further enhanced by an atomic-force-microscope tip, to realize a FE switch [21]. Usually, the time required for such a switch is long, even longer than those made by directly applying an electric pulse. This is because of the limitations set by conventional nucleation-growth process and domain-wall movement. In contrast, a coherent light can cause a phase transition/switch in a much shorter time [22–25]. However, how to realize such an optically induced ultrafast nonvolatile FE switch is still a challenging task, as an ultrafast order-to-order transition/switch in a memory material alone would not be enough unless one can also demonstrate the nonvolatility of the process.

In this paper, we show that the FE switch could in principle be controlled with precision, which points to the direction of optical ultrafast nonvolatile memory. The following three factors are important for realizing the control: (1) a lowering of the transition energy barrier to a threshold as a result of the optical excitation, (2) a coherent directional motion of the atoms as a result of the coherence of the laser light, and (3) most importantly there exists an effective electron-phonon

---

*These authors contributed equally to this work.
†lixianbin@jlu.edu.cn
‡hbsun@tsinghua.edu.cn
§zhangs9@rpi.edu

coupling in the memory material that can prevent the switch-back of the polarization. Time-dependent density-functional theory molecular dynamics (TDDFT MD) calculations reveal ultrafast nonvolatile FE switches in both binary GeTe and ternary PbTiO$_3$.

II. METHOD

Ground-state molecular dynamics (MD) was carried out based on the density-functional theory (DFT) and a canonical ensemble (*NVT*) using the SIESTA code [26]. The time step is 3 fs for GeTe and 2 fs for PbTiO$_3$. Excited-state MDs were carried out based on the time-dependent density-functional theory (TDDFT), as implemented in the SIESTA code [27]—a technique that can describe real-time nonadiabatic electron-phonon, electron-electron couplings, and the change of the lattice under excitation [27–29]. Here, a microcanonical ensemble (*NVE*) and a time step of 0.024 fs were used. The equilibrium state of ground-state MD at 300 K was adopted as the input to TDDFT MD. Norm-conserving Troullier-Martins pseudopotentials [30], the Perdew-Burke-Ernzerhof (PBE) exchange-correlation functional [31], and the local basis sets with double-ζ polarized orbitals were employed. In generating the pseudopotentials, the valence electron configurations of Ge [$4s^2 4p^2$], Te [$5s^2 5p^4$], Pb [$5d^{10} 6s^2 6p^2$], Ti [$3d^2 4s^2$], and O [$2s^2 2p^4$] were used. The energy cutoffs for the plane wave expansion were 100 Ry for GeTe and 350 Ry for PbTiO$_3$. A 192-atom supercell for rhombohedral GeTe (*r*-GeTe) and a 135-atom supercell for tetragonal PbTiO$_3$ (*t*-PbTiO$_3$) were used in both the ground-state and excited-state MDs with the Γ point for Brillouin zone integration. The excitation was simulated by elevating electrons from the valence band maximum (VBM) to the conduction band minimum (CBM). The excitation intensity is given in percentage of the total number of valence electrons. More details of the TDDFT-MD method can be found in the Supplemental Material [32].

III. RESULTS AND DISCUSSION

Most ferroelectric materials are displacive ferroelectrics [7,8,33], in which the electric polarization is governed by the displacements of atoms along a certain direction. The origin of the spontaneous polarization can be attributed to a Peierls distortion or a pseudo-Jahn-Teller distortion of the crystal [34,35]. Optical excitation changes the potential-energy surfaces (PESs), thereby offering the ability to control the ferroelectric polarization. Taking the binary ferroelectric GeTe as an example, here we elucidate the physics behind the FE switch by light. Figure 1 shows the calculated PES as a function of the position of the Ge atoms, which are coherently displaced relative to the Te atoms along the *z* axis or [001] direction, which is also the direction of its polarization *P*. The double-well PES is characteristic of ferroelectricity with the *P*'s at the two energy minima pointing in opposite directions. In the ground state, a switching between the two energy minima is prevented by the relatively large transition energy barrier in Fig. 1.

Upon an above-gap laser excitation, which alters the occupation of the states, the energy barrier is reduced, as can be
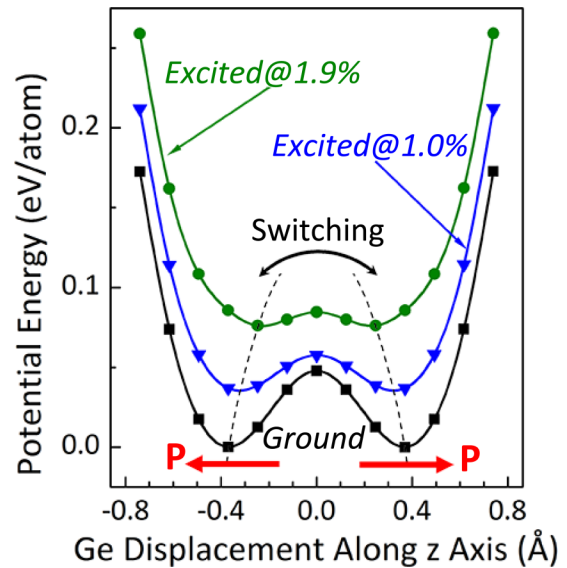

FIG. 1. Potential-energy surfaces of ferroelectric *r*-GeTe as a function of Ge displacement. Black, blue, and green lines and symbols are the PESs of the ground state, and the excited states with 1.0% and 1.9% excitations, respectively. Dashed lines indicate the positions of the energy minima, whereas red arrows indicate the directions of the polarization (*P*). In these calculations, electronic occupations are fixed for respective excitations.

seen in Fig. 1. The excitation also alters the PES from that of the ground state, thereby effectively inserting forces on the atoms. These forces are coherent and hence directional in the *z* direction: e.g., for a system originally equilibrated at the left energy minimum in Fig. 1, the predominant forces on the Ge atoms would all point to the right. To conserve momentum, forces on the Te atoms must all point to the opposite direction. At a threshold laser intensity, which is calculated to be about 1.9% for *r*-GeTe (i.e., 1.9% total valence electrons are excited to the conduction band), these atoms will overcome the reduced barrier so an FE switch takes place. For an ultrafast laser, 1.9% excitation is considered modest and is far below the melting point of the crystal.

Figures 2(a) and 2(b) show schematically two local atomic motifs (centered on a Ge atom) before and after the FE switch, which are characterized by the existence of both long and short bonds. An FE switch constitutes a switching of all the long bonds to short bonds, and vice versa. Figures 2(c) and 2(d) show the average long and short bond lengths as a function of time, given by a 300-K TDDFT-MD run. At 0% excitation in Fig. 2(c), we see no sign of bond switching except some thermal fluctuation. At the threshold excitation, on the other hand, we see in Fig. 2(d) that the long bonds have all become short bonds while the short bonds have all become long bonds in less than 1 ps. For nonvolatile memory, the polarization state after the FE switch must be kept unchanged. This is indeed the case in Fig. 2(d) where the newly formed long and short bonds oscillate around their respective new equilibrium positions (see Fig. 1) with attenuating amplitudes. We note that the observed FE switch is a robust phenomenon. Extra TDDFT-MD simulations with different initial input structures at 300 K in Fig. S1 of the Supplemental Material
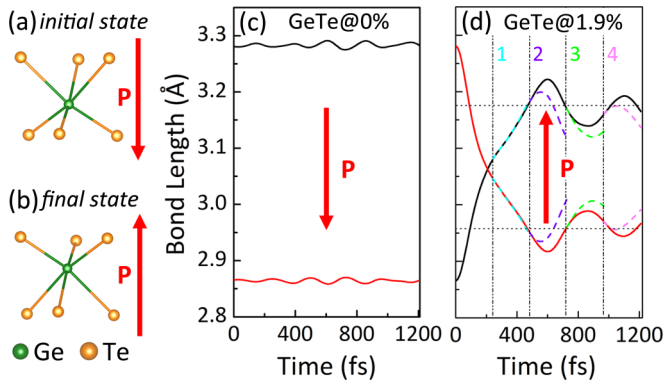
FIG. 2. Schematic illustrations of Ge-centered motifs (a) before and (b) after the switching. As in Fig. 1, P is the polarization. Time evolutions of long/short bonds during (c) the ground-state MD and (d) TDDFT MD with 1.9% excitation. The dashed curves indicate the results of electronic occupation resets to 0 fs. Vertical dash-dot-dot lines in (d) indicate the time of the reset excitation. Horizontal dotted lines in (d) indicate the positions of energy minima at this excitation.

[32] show the same switching. Meanwhile, there also exists a controllable excitation-intensity window for the FE switch; see Fig. S2 of the Supplemental Material [32].

Evidently, the attenuation of the oscillations is most critical for nonvolatile memory. To understand its physics, Fig. 3(a) shows the time evolution of average momenta for Ge and Te at the threshold excitation. As can be seen from the figure, in the early stage of the MD [within 70 fs], there is a gain in the magnitude of momenta along the z axis for both Ge and Te, which is responsible for the atoms collectively overcoming the reduced energy barrier at a later time of approximately 200 fs in Fig. 2(d). The (x, y) in-plane momenta, which are characteristic of a random thermal motion, also develop but at a significantly later time. At this point, the z-axis momentum may also lose its coherency. Energy is conserved in our TDDFT-MD simulation. Hence, as the coherent motion along the z axis ceases, the system loses the directional driving force to switch back.

We stress the critical importance of the coherence: a high coherence, or being in phase, of the electronic states promotes the FE switch, while a prompt dephasing prevents it from switching back. To see the former, consider the case where only a single Ge atom is displaced along the z axis, while all other atoms are fixed at their ground-state positions. Figures 3(b) and 3(c) show the PESs for the ground state and at 1.9% threshold excitation. It is clear that in the absence of a coherent motion of the atoms, the second energy minimum in Fig. 1 disappears so the displaced Ge is always pushed back to its original position. To see the latter, on the other hand, we reset the occupation of the excited carriers at a later t to that at $t = 0$. If the system electronic states have not significantly evolved with time, the reset would have negligible effect on the atomic trajectory and hence on the evolution of the bond lengths. Figure 2(d) shows in dashed line the results with four resets from which we determine the dephasing time for r-GeTe to be approximately 500 fs. The physical causes for the dephasing are electron-electron, electron-phonon, and phonon-phonon scatterings. The rate
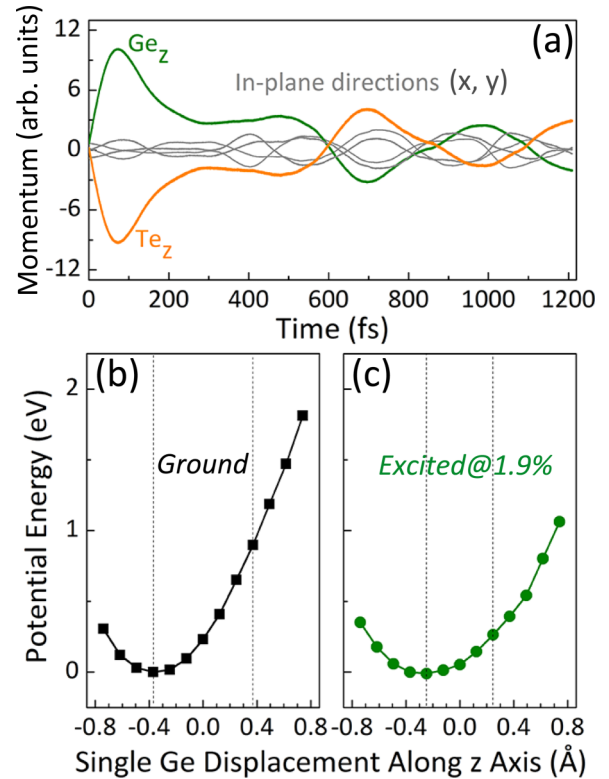

FIG. 3. (a) Time evolution of average momenta of Ge and Te along the (x, y, z) directions in r-GeTe with 1.9% excitation. The PESs of a single Ge atom (b) in the ground state and (c) with the 1.9% excitation. In these calculations, all other atoms are fixed at their ground-state positions. Vertical dotted lines indicate the positions of the two energy minima in Fig. 1 where all other atoms are allowed to relax.

of electron-phonon scattering is critically important not only because once a noticeable portion of the energy is taken away by phonons, the excitation energy is below the required threshold, but also the increased phonon-phonon scattering (as a result of increased phonon population) will destroy the coherent motion of the atoms.

The physics above is general and by no means applies only to ferroelectric binary GeTe. As a matter of fact, it also applies to regular perovskite-type ferroelectric ternary $PbTiO_3$. To see this, Figs. 4(a) and 4(b) show the local structural motifs (centered on an O atom) for a t-$PbTiO_3$ before and after the FE switch similar to those in Fig. 2. Unlike GeTe, however, here there are two types of long and short bonds: i.e., the Pb-O and Ti-O bonds, respectively. Figures 4(c) and 4(d) show the time evolutions of these bonds in the ground state and with a 1.6% threshold excitation. In spite of the general complexity associated with the coexistence of Pb^{+2} and Ti^{+4} cations, here a nonvolatile FE switch is achieved within 800 fs with the excitation. Figure 4(e) shows the calculated partial density of states (PDOS). It reveals that, for the optical FE switch, Ti atoms play a more important role than Pb atoms. This is because the states involved in the excitation are mainly Ti d and O p states, as can be seen in the real-space distributions of the valence band maximum (VBM) state in Fig. 4(f) and conduction band minimum (CBM) state in Fig. 4(g). More
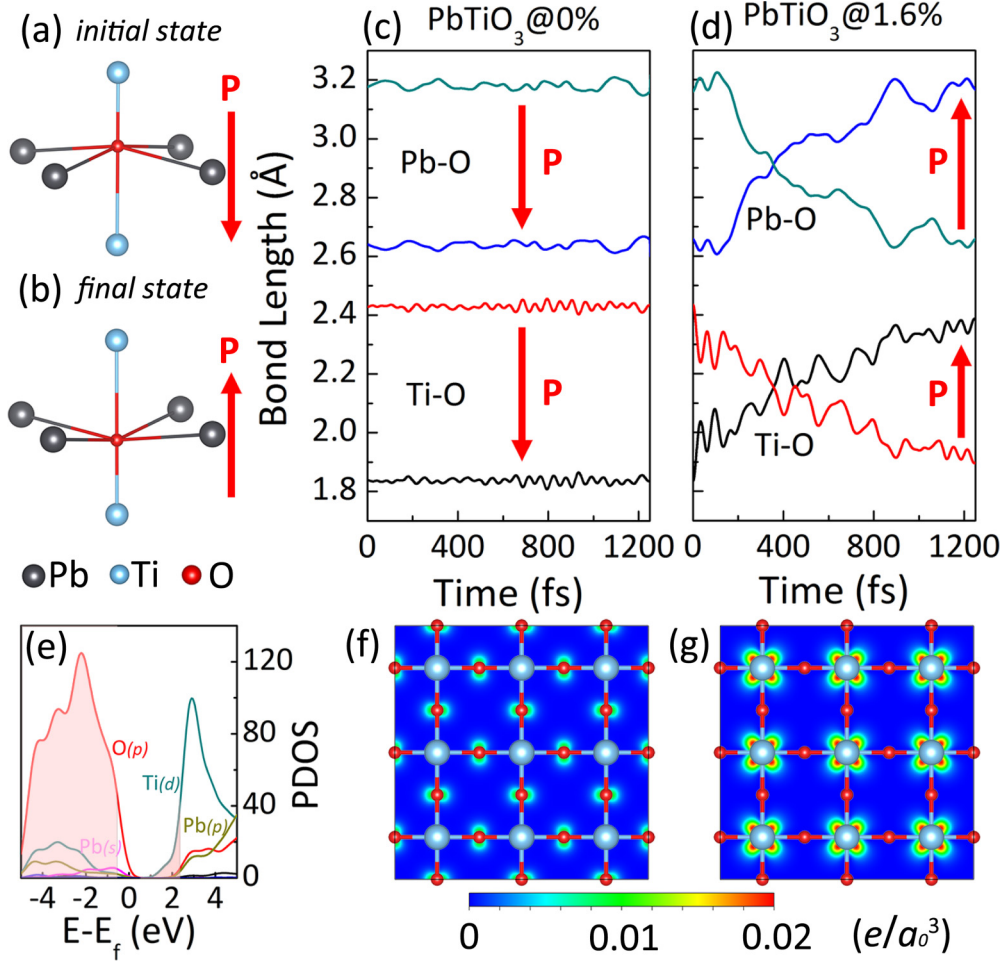
FIG. 4. Excitation-induced FE switch in ferroelectric t-PbTiO$_3$. Schematic illustrations of O-centered motifs (a) before and (b) after the switching. Time evolutions of long/short bonds of Pb-O and Ti-O during (c) the ground-state MD and (d) TDDFT MD with 1.6% excitation. (e) Partial density of states (PDOS) where electron occupation upon the excitation is given by shading. Projected charge densities for (f) the VBM and (g) CBM in unit of e/a_0^3, where a_0 is the Bohr radius.

generally, optical switching between bistable states has been demonstrated for other systems, noticeably between charge density wave states of In nanowire on Si(111) in a recent experiment [36]. The similarity of the phenomena suggests that the same physics apply.

The rate of the electron-phonon scattering is clearly material dependent. Hence, not every ferroelectric material is necessarily suitable for a nonvolatile FE switch. For example, our study shows that BaTiO$_3$ would switch back at approximately 240 fs. One could perceivably adjust the ambient conditions to alter the rate of scattering, thereby preventing the switchback. For example, for the aforementioned charge density wave states of In nanowire, a superb cooling property of the substrate, which may be viewed as an ambient, has been attributed to the effective blocking of switchback [37].

It should also be noted that in our study excitonic effects are negligible. This is because of the high density of carriers (on the order of $10^{21}/cm^3$ in this work). The metallic screening by the excited carriers drastically reduces the exciton binding energy to result in a transition from an insulating excitonic phase to a dense electron-hole plasma. In fact, such a transition has been experimentally observed in ZnO [38] with a relatively large exciton binding energy: For example, ultrafast spectroscopy study has revealed a complete quench of the exciton resonance when the excited electron-hole concentration exceeds $7 \times 10^{18}/cm^3$.

IV. CONCLUSIONS

In summary, we develop the physics for an ultrafast nonvolatile FE switch by coherent laser. Compared with mechanisms deployed for nonvolatile memory without lights, coherent atomic motion induced by the coherent light can increase the speed of writing by $-$two to three orders of magnitude and shorten the writing time to subpicoseconds. Most importantly, we established the criterion for nonvolatility, namely, the rate for dephasing due to the electron-phonon scattering to deter a switchback, which is largely a property of the material but to a smaller degree may also rely on the ambient. Detailed TDDFT-MD calculations reveal that both GeTe and PbTiO$_3$ fulfill the requirements to realize an ultrafast nonvolatile FE switch.

[1] B. J. Choi, A. C. Torrezan, K. J. Norris, F. Miao, J. P. Strachan, M. X. Zhang, D. A. Ohlberg, N. P. Kobayashi, J. J. Yang, and R. S. Williams, Nano Lett. **13**, 3213 (2013).

[2] J. Li, B. Nagaraj, H. Liang, W. Cao, C. H. Lee, and R. Ramesh, Appl. Phys. Lett. **84**, 1174 (2004).

[3] F. Rao, K. Ding, Y. Zhou, Y. Zheng, M. Xia, S. Lv, Z. Song, S. Feng, I. Ronneberger, R. Mazzarello, W. Zhang, and E. Ma, Science **358**, 1423 (2017).

[4] G. E. Rowlands, T. Rahman, J. A. Katine, J. Langer, A. Lyle, H. Zhao, J. G. Alzate, A. A. Kovalev, Y. Tserkovnyak, Z. M. Zeng, H. W. Jiang, K. Galatsis, Y. M. Huai, P. K. Amiri, K. L. Wang, I. N. Krivorotov, and J. P. Wang, Appl. Phys. Lett. **98**, 102509 (2011).

[5] N. Yamada, Phys. Status Solidi B **249**, 1837 (2012).

[6] J. F. Scott, Ferroelectrics **503**, 117 (2016).

[7] M. Dawber, K. M. Rabe, and J. F. Scott, Rev. Mod. Phys. **77**, 1083 (2005).

[8] L. W. Martin and A. M. Rappe, Nat. Rev. Mater. **2**, 16087 (2016).

[9] T. Choi, S. Lee, Y. J. Choi, V. Kiryukhin, and S. W. Cheong, Science **324**, 63 (2009).

[10] D. Daranciang, M. J. Highland, H. Wen, S. M. Young, N. C. Brandt, H. Y. Hwang, M. Vattilana, M. Nicoul, F. Quirin, J. Goodfellow, T. Qi, I. Grinberg, D. M. Fritz, M. Cammarata, D. Zhu, H. T. Lemke, D. A. Walko, E. M. Dufresne, Y. Li, and J. Larsson *et al.*, Phys. Rev. Lett. **108**, 087601 (2012).

[11] S. Y. Yang, J. Seidel, S. J. Byrnes, P. Shafer, C. H. Yang, M. D. Rossell, P. Yu, Y. H. Chu, J. F. Scott, J. W. Ager, 3rd, L. W. Martin, and R. Ramesh, Nat. Nanotechnol. **5**, 143 (2010).

[12] B. Kundys, M. Viret, D. Colson, and D. O. Kundys, Nat. Mater. **9**, 803 (2010).

[13] C. Paillard, B. Xu, B. Dkhil, G. Geneste, and L. Bellaiche, Phys. Rev. Lett. **116**, 247401 (2016).

[14] F. Rubio-Marcos, A. Del Campo, P. Marchet, and J. F. Fernandez, Nat. Commun. **6**, 6594 (2015).

[15] W. L. Warren and D. Dimos, Appl. Phys. Lett. **64**, 866 (1994).

[16] R. Guo, L. You, Y. Zhou, Z. S. Lim, X. Zou, L. Chen, R. Ramesh, and J. Wang, Nat. Commun. **4**, 1990 (2013).

[17] C. Y. J. Ying, A. C. Muir, C. E. Valdivia, H. Steigerwald, C. L. Sones, R. W. Eason, E. Soergel, and S. Mailis, Laser Photonics Rev. **6**, 526 (2012).

[18] H. Steigerwald, Y. J. Ying, R. W. Eason, K. Buse, S. Mailis, and E. Soergel, Appl. Phys. Lett. **98**, 062902 (2011).

[19] T. Li, A. Lipatov, H. Lu, H. Lee, J. W. Lee, E. Torun, L. Wirtz, C. B. Eom, J. Iniguez, A. Sinitskii, and A. Gruverman, Nat. Commun. **9**, 3344 (2018).

[20] F. Rubio-Marcos, D. A. Ochoa, A. Del Campo, M. A. García, G. R. Castro, J. F. Fernández, and J. E. García, Nat. Photonics **12**, 29 (2018).

[21] M. M. Yang and M. Alexe, Adv. Mater. **30**, 1704908 (2018).

[22] N.-K. Chen, X.-B. Li, J. Bang, X.-P. Wang, D. Han, D. West, S. Zhang, and H.-B. Sun, Phys. Rev. Lett. **120**, 185701 (2018).

[23] C. Lian, Z. A. Ali, H. Kwon, and B. M. Wong, J. Phys. Chem. Lett. **10**, 3402 (2019).

[24] T. Qi, Y. H. Shin, K. L. Yeh, K. A. Nelson, and A. M. Rappe, Phys. Rev. Lett. **102**, 247603 (2009).

[25] A. Subedi, Phys. Rev. B **92**, 214303 (2015).

[26] J. M. Soler, E. Artacho, J. D. Gale, A. Garcia, J. Junquera, P. Ordejon, and D. Sanchez-Portal, J. Phys.: Condens. Matter **14**, 2745 (2002).

[27] S. Meng and E. Kaxiras, J. Chem. Phys. **129**, 054110 (2008).

[28] J. Bang, Y. Y. Sun, X. Q. Liu, F. Gao, and S. B. Zhang, Phys. Rev. Lett. **117**, 126402 (2016).

[29] E. Runge and E. K. U. Gross, Phys. Rev. Lett. **52**, 997 (1984).

[30] N. Troullier and J. L. Martins, Phys. Rev. B **43**, 1993 (1991).

[31] J. P. Perdew, K. Burke, and M. Ernzerhof, Phys. Rev. Lett. **78**, 1396 (1997).

[32] See Supplemental Material at http://link.aps.org/supplemental/10.1103/PhysRevB.102.184115 for the detailed explanation of the real-time TDDFT-MD method, discussion of initial input structures for the FE switch, and discussion of the excitation-intensity window for the FE switch.

[33] N. Setter, D. Damjanovic, L. Eng, G. Fox, S. Gevorgian, S. Hong, A. Kingon, H. Kohlstedt, N. Y. Park, G. B. Stephenson, I. Stolitchnov, A. K. Taganstev, D. V. Taylor, T. Yamada, and S. Streiffer, J. Appl. Phys. **100**, 051606 (2006).

[34] G. S. Pawley, W. Cochran, R. A. Cowley, and G. Dolling, Phys. Rev. Lett. **17**, 753 (1966).

[35] V. Polinger, P. Garcia-Fernandez, and I. B. Bersuker, Physica B (Amsterdam, Neth.) **457**, 296 (2015).

[36] T. Frigge, B. Hafke, T. Witte, B. Krenzer, C. Streubuhr, A. Samad Syed, V. Miksic Trontl, I. Avigo, P. Zhou, M. Ligges, D. von der Linde, U. Bovensiepen, M. Horn-von Hoegen, S. Wippermann, A. Lucke, S. Sanna, U. Gerstmann, and W. G. Schmidt, Nature **544**, 207 (2017).

[37] Private conversation between Shengbai Zhang and Wolf Gero Schmidt.

[38] T. Shih, E. Mazur, J. P. Richters, J. Gutowski, and T. Voss, J. Appl. Phys. **109**, 043504 (2011).